

To be submitted to  
Nucl. Instr. & Meth.

ISTITUTO NAZIONALE DI FISICA NUCLEARE  
Laboratori Nazionali di Frascati

LNF-81/68(P)  
28 Novembre 1981

G. Bologna, F. Celani, A. Codino, B. D'Ettorre Piazzoli, F.L. Fabbri,  
M. Giardoni, P. Laurelli, G.P. Mannocchi, P. Picchi, G. Rivellini, L.  
Satta, P. Spillantini and A. Zallo: A SET OF MULTIGAP PLANE  
PROPORTIONAL CHAMBERS WITH OPTIMIZED SENSITIVITY SUR-  
FACE FOR A VERTEX DETECTOR

LNF-81/68(P)  
28 Novembre 1981

## A SET OF MULTIGAP PLANE PROPORTIONAL CHAMBERS WITH OPTIMIZED SENSITIVE SURFACE FOR A VERTEX DETECTOR

F. Celani, A. Codino, F.L. Fabbri, M. Giardoni, P. Laurelli, G. Rivellini, L. Satta, P. Spillantini, A. Zallo  
INFN - Laboratori Nazionali di Frascati, Frascati, Italy

and

G. Bologna, B. D'Ettorre Piazzoli, G.P. Mannocchi, P. Picchi  
Istituto di Fisica and Laboratorio di Cosmogeofisica del CNR, Torino, Italy

### ABSTRACT

The construction and performance of multigap plane MWPC's  $108 \times 108 \text{ cm}^2$  are described. Relevant details on the construction procedure and the results of operating tests are reported. These chambers are operating in the NA1 experiment at SPS, CERN.

### 1. - INTRODUCTION

We describe a set of MWPC's of  $1.16 \text{ m}^2$  useful surface, used in the NA1 experiment at SPS, CERN to measure the lifetime of charmed mesons in a purely electronic way<sup>(1)</sup> for the first time. The apparatus consists of a forward spectrometer covering the angular region between  $0^\circ$  and  $6^\circ$  and a multilayer active silicon target surrounded by a vertex detector. The vertex detector is composed of a drift chambers box, a set of MWPC's and a segmented photon detector. (Fig. 1).

In the vertex detector design we had to solve the problem of getting the maximum number of information preserving the physical dimensions of the whole detector to a reasonable size. In a volume of less than  $1 \text{ m}^3$  we installed  $\sim 200$  drift cells,  $\sim 3000$  proportional wires and  $\sim 500$  pm's, ensuring the complete coverage for charged particles up to  $120^\circ$  and the detection and energy measurement of photons up to  $70^\circ$ .

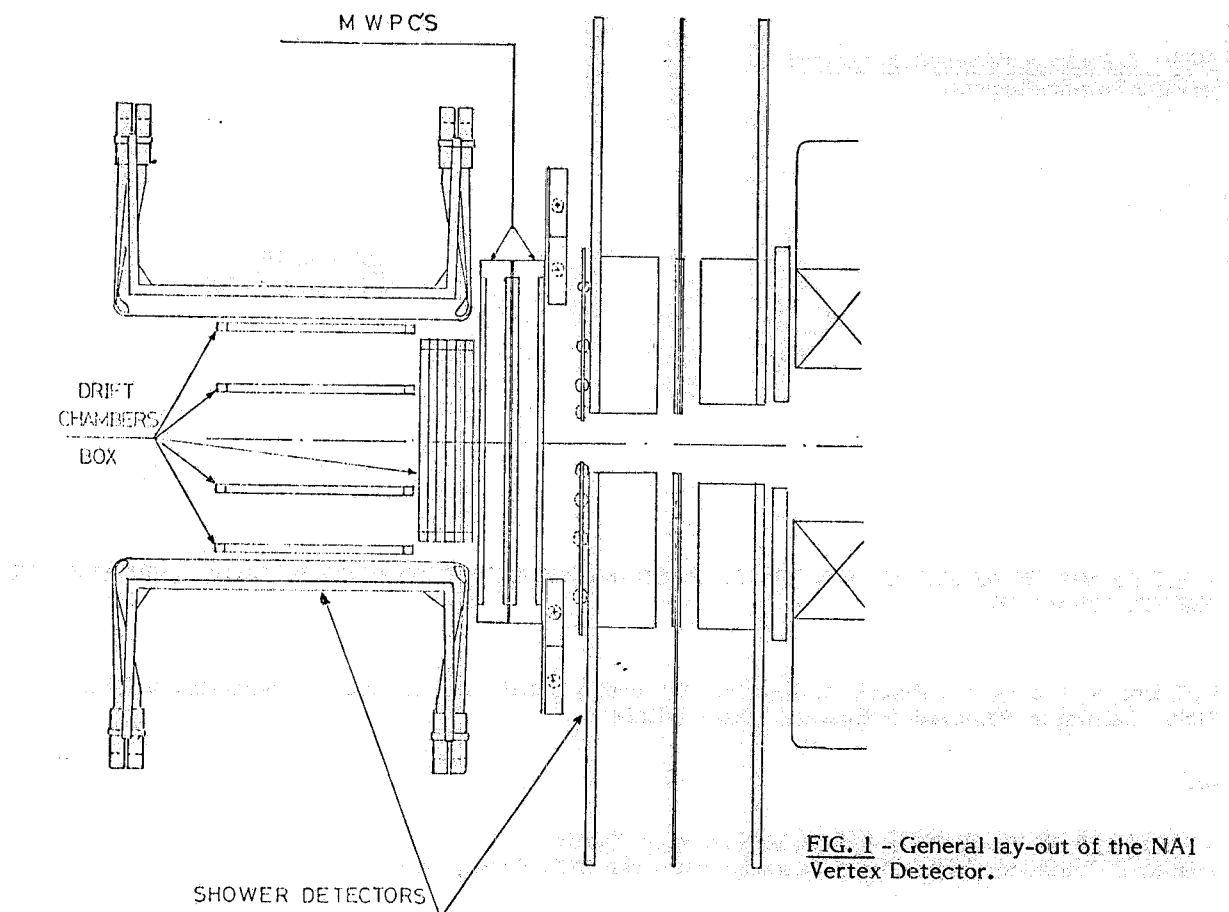


**FIG. 1 - General lay-out of the NA1 - Vertex Detector.**

The MWPC's were used for triggering purposes and off line analysis. The main requirements on the MWPC's were that, independently from the drift chambers information, the interaction point should be reconstructed with a precision better than 2 mm in the direction perpendicular to the beam, and that the secondary vertexes due to K and  $\Lambda$  decays should be identified. All these conditions had to be satisfied by a MWPC set less than 20 cm thick, since the compactness of the vertex detector did not allow a longer lever arm.

In the present paper we describe the characteristics of the MWPC design, the construction procedure and we report the performance of the MWPC's in the test runs and in the NA1 data acquisition runs.

## 2. - DESIGN AND CONSTRUCTION

The design was mainly influenced by the request of having the minimum depth in the beam direction. Accordingly, we decided to build the chambers with three sense wires planes (instead of two, as usual) to reduce the total number of external support frames. In order to decouple optically the gaps, we used for the cathode planes aluminium foils 40 micron thick. Because of this choice we were forced to maintain the overall mechanical tolerance at the 1% level to prevent high voltage breakdown in the chambers.

The main mechanical characteristics of the chambers are: a)  $108 \times 108 \text{ cm}^2$  internal dimension, b) 20 micron wires, c) 2 mm pitch, d) 8 mm gap. Each chamber is composed of eight vetronite frames (Stesalit 4411W), held together by two aluminium frames, ensuring the necessary mechanical rigidity. On the frames are glued two aclar foils 50 micron thick for gas enclosure (Fig. 2).

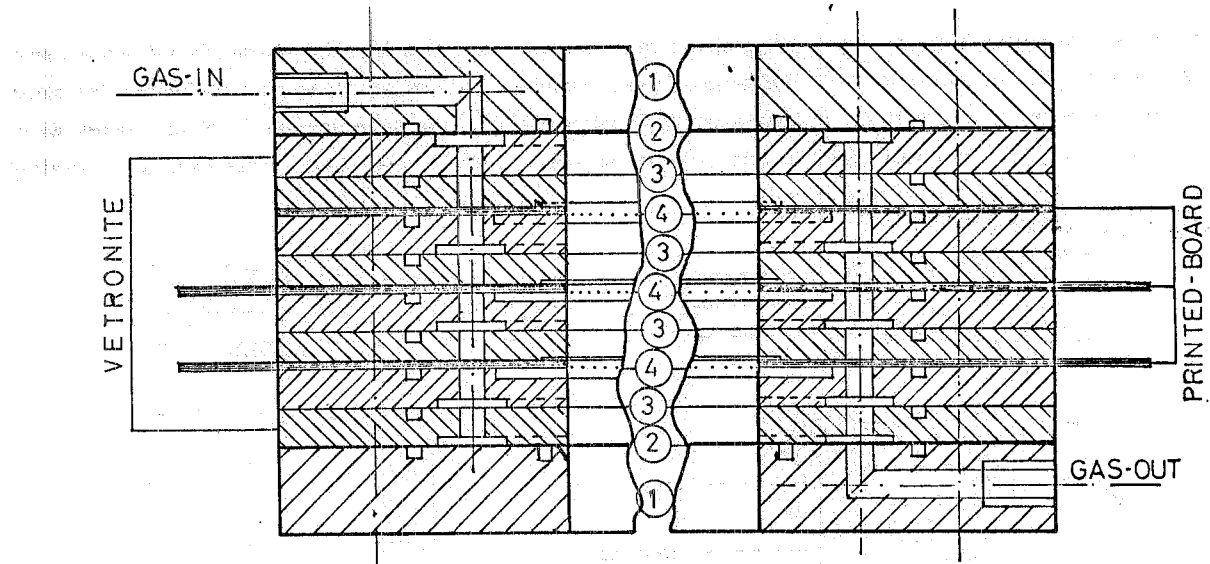


**FIG. 2** - Cross view of a single multiwire proportional chamber. 1) external aluminium frame, 2) aclar window, 3) cathode aluminium foil, 4) sense wires. The sense wires are indicated by dots on the three planes.

#### a) Cathode planes

To limit to 0.1 mm the dishing-in of the cathode due to the electrostatic force, the aluminium foils have to be stretched before being glued on the frames. To this purpose the foils are laid out on a specially designed table where they can be heated to 40°C and stretched by means of the atmospheric pressure, making a moderate vacuum in a grove milled along the rim of the table. The foils are heated mainly to speed up the glue polymerization. The size of the grove is determined from the solution of the differential equation describing a membrane deformed by a distributed force. In our case, at the center of the cathode plane, the solution is of the form

$$u(0,0) = \frac{pL^2}{8T} \left[ 1 - \frac{32}{\pi^3} \sum_{k=0}^{\infty} \frac{(-1)^k}{(2k+1)^3 \cos h(2k+1) \frac{\pi}{2}} \right] \approx 7.37 \times 10^{-2} \frac{P}{T} L^2$$

where  $p$  is the electrostatic pressure,  $L^2$  the surface of the aluminium foil and  $T$  the mechanical stress.

By imposing that the maximum vertical displacement be less than 0.1 mm, one can calculate the corresponding mechanical stress that must be applied to the aluminium foil. Since the stress due to the heating is insufficient, the size of the grove has to be such that the total force per meter equals the computed mechanical stress. Finally, to provide additional path length for surface discharges, mylar strips 10 mm wide and 250 micron thick are inserted over and under the cathode in a slot, cut in the inner perimeter of the vetronite frames.

#### b) Wire Planes

The wires are stretched to  $50 \pm 0.5$  g. They are soldered on the printed board and glued with araldite for maximum safety. The three sense planes are oriented in different directions: two of them scan the horizontal and vertical coordinates, while the third one is oriented at  $45^\circ$  for ambiguity resolution. Due to the dimension of the chamber, the wires have to be supported. To avoid inefficiencies in the central region we stretched for each

plane two copper wires, insulated by a teflon sleeve of 1 mm diameter, in a direction normal to the sense wires, at +20 cm and -20 cm with respect to the centre of the chamber. The copper wires over and under the sense wires are tied together every 10 cm by means of a thin nylon thread. The fastening details of the copper wires are reported in Fig. 3. To smooth the electric field at the edge, the last three sense wires have an increasing diameter: 40,75 and 100 micron respectively.

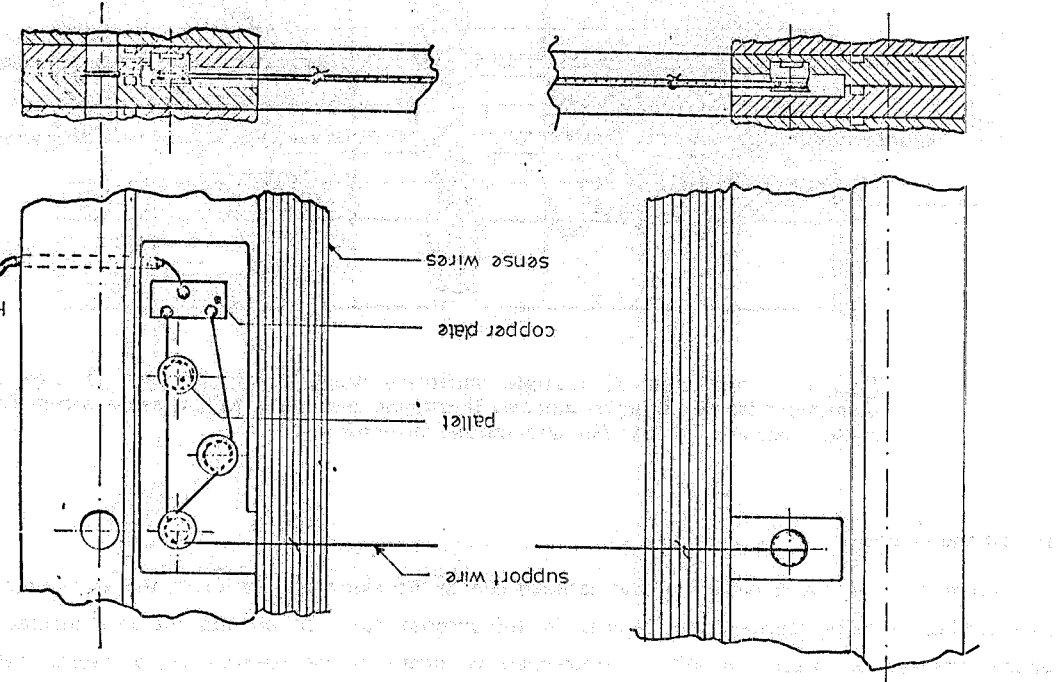


**FIG. 3 -** Fastening details (side and cross views). The pallet where the copper wire is anchored is glued in a hole drilled in the vetroneite frame. The small slab where the copper wire is soldered is made of copper and the correcting voltage is fed through a cable running to the exterior.

### c) Gas Flow

For space reasons, the gas inlet and outlet are drilled in the aluminium frame in the direction of the wire planes. Since the three gaps do not communicate due to the cathode foils, the gas is brought to the gap through holes in the vetroneite frames. The entrance to each gap is obtained by milling several rectangular openings in the vetroneite, to obtain a gas flow as uniform as possible.

It is to be noted that the vetroneite frames are not sufficiently rigid to support the stress of the wire planes or the aluminium foils without severe deformations.

During the operation of the chambers the mechanical rigidity is provided by the external aluminium frames, on which each plane is fixed in the assembling procedure. When a chamber is opened each plane is screwed to an independent supporting frame which sustains the mechanical stress. In this way the assembly procedure is rather cumbersome, but it guarantees the requested tolerance.

### 3.1 - ELECTRONICS AND TESTS

The readout we used was originally designed by Lindsay et al.<sup>(2)</sup>. We had to redesign the preamplifiers to have the possibility of stacking them on the chambers. They are protected against sparks by 1.8 KOhm resistors soldered on the printed board circuit of the chamber.

The high voltage generator has been especially designed for the NAI vertex detector chambers and was described elsewhere<sup>(3)</sup>. Its main features are that it is located near the chambers and is remotely controlled by the on-line computer. The maximum current it can draw is hardware prefixed to a value depending on the beam intensity. If a voltage breakdown occurs in the chamber, the generator automatically drops the high voltage in nearly one millisecond to a point where the current falls below the fixed value. This way the chambers are protected against multiple sparking.

During tests and data taking we always used the so called magic gas mixture (isobutane 25%, freon 13B1 0.1%, methylal 5% in argon). In nearly one year of operation we did not observe any deterioration of chamber performances. We only noted on the cathode planes a white spot in the beam region.

The chambers were tested in a laboratory with a  $^{106}\text{Ru}$  source and with a pion beam at the CERN PS. Fig. 4 shows the efficiency curve of the three wire planes in the central region, obtained with 10 GeV/c pions. The

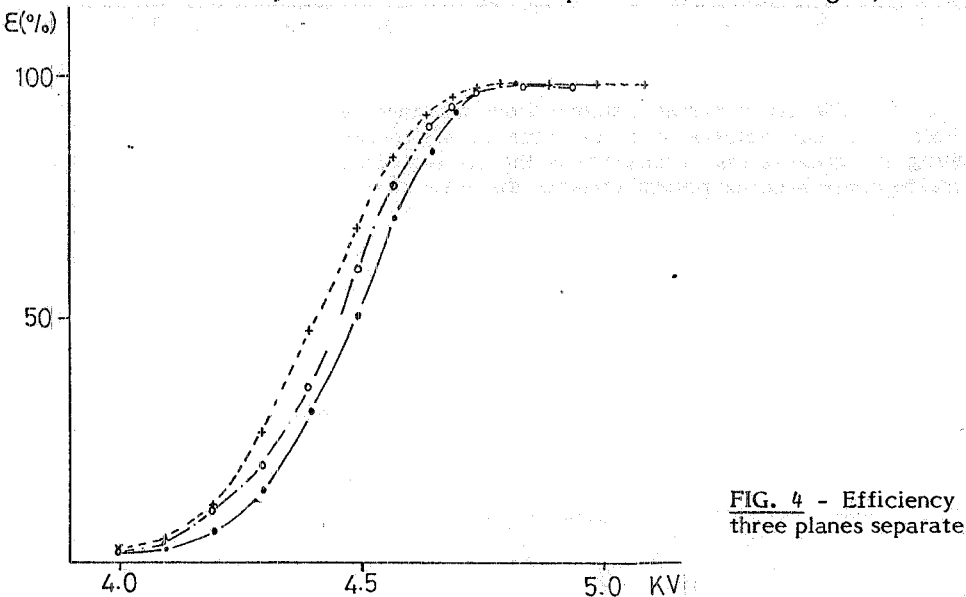


FIG. 4 - Efficiency versus high voltage for the three planes separately.

point of inflection of the curves lies in a  $\sim 100$  V range, and the plateau extends for a few hundreds volts. Inside the plateau zone the mean multiplicity for normal incidence varies between 1.1 and 1.2 for the three planes. Similar results were obtained with the  $^{106}\text{Ru}$  source, and we also noted the existence of a plateau in the singles counting rate of the planes. After a careful conditioning of the chambers, carried out by increasing the high voltage in such a way that the dark current is limited to  $5 \mu\text{A}$ , and waiting for it to return to zero before a new voltage increment, the final noise rate, 100 V after the highest plateau knee was a few Hz per wire.

Concerning the efficiency uniformity over the whole chamber surface, the measurements performed are within 3% of the value of the central region.

Figs. 5a) and b) show the efficiency variation near the edge of the chambers, in a direction perpendicular and parallel to the wires, respectively. The arrows indicate the position of the mylar strips. The two curves are rather similar, and the full efficiency is reached about 12 mm from the mylar strips. In Fig. 6 the efficiency

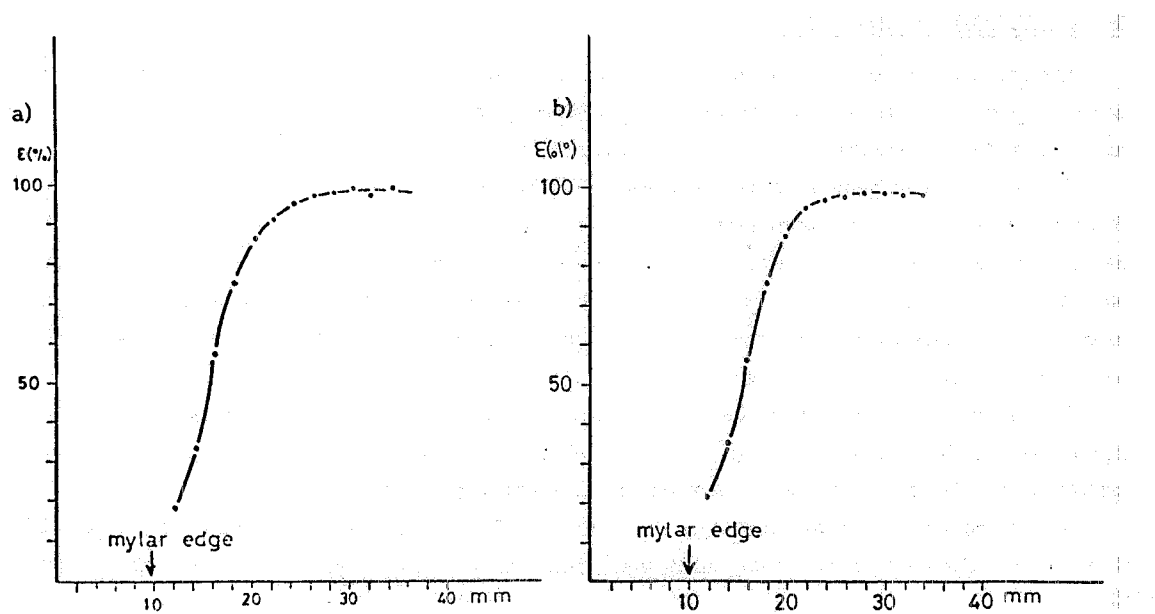


FIG. 5 - Efficiency versus distance from the edge. a) Abscissa is the distance from the edge in a direction along the sense wires; b) abscissa is the distance from the edge in a direction perpendicular to the sense wires.

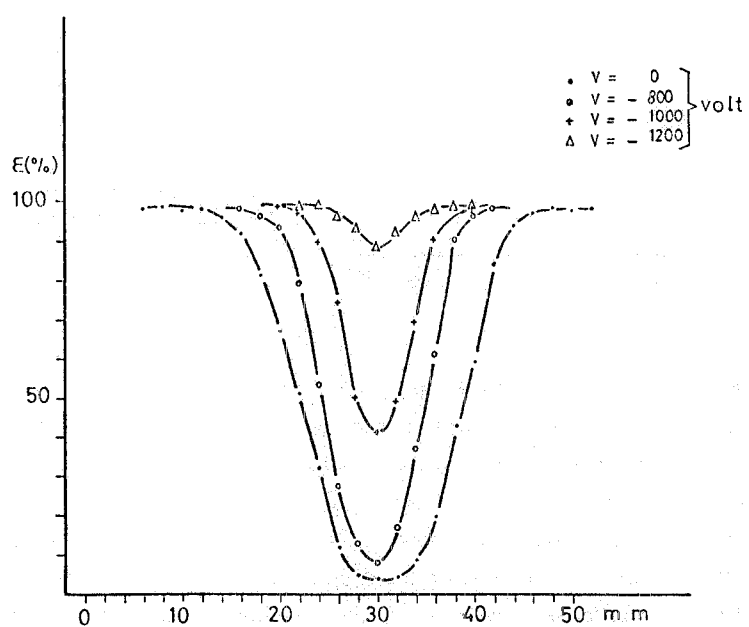


FIG. 6 - Efficiency around the support wires for various correcting voltages.

around the support wire, for various voltages, is reported. The measured points are spaced by 2 mm. At 1.4 KV the width of the inefficiency zone is reduced below the sensitivity of the measurement procedure. In fact, if the FWHM of these zones is plotted versus the high voltage, the extrapolation of the resulting straight line to 1.5 KV gives a width of less than one millimeter. The efficiency of a sense wire on the support wires, is reported in Fig. 7 versus the high voltage, and shows that a plateau zone is slowly reached.

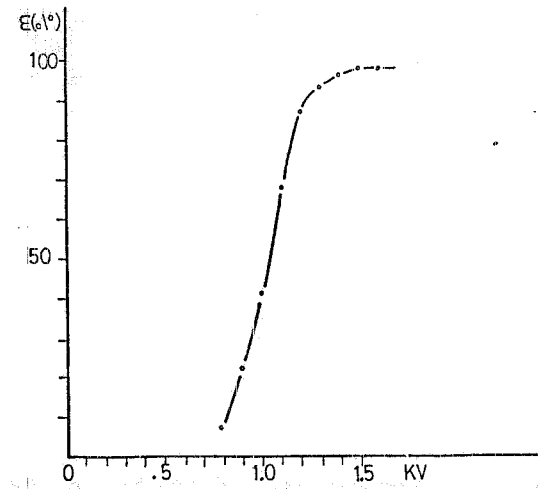


FIG. 7 - Efficiency curve around the support wire as a function of the correcting voltage at an operating voltage of 5 KV.

Hereafter we report some results in the analysis of data of the NA1 experiment obtained with these chambers. One of the most important items where the chambers are essential is the determination of the primary and secondary vertexes of the events. Fig. 8 shows the x and y vertex projections for a sample of

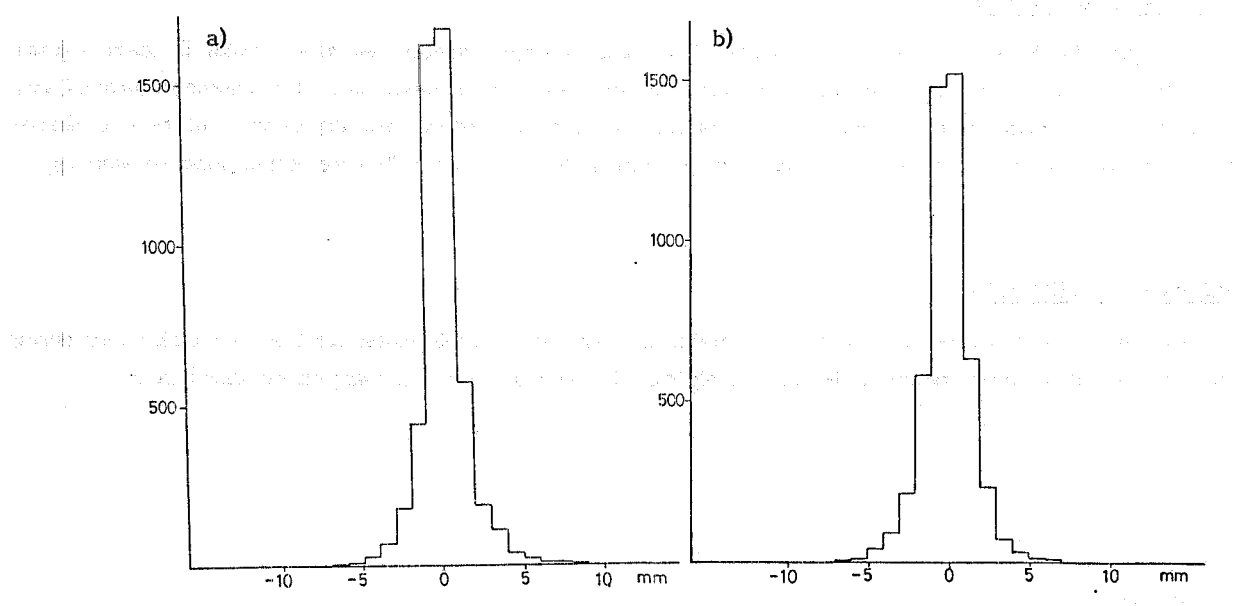


FIG. 8 - X (a) and Y (b) vertex projections determined by means of all traces reconstructed in the MWPC's.

~5000 events, determined by using all the straight lines reconstructed in the MWPC's. If one rejects, event by event, all traces which pass at a distance from this vertex greater than a suitable cut, the remaining ones define the primary vertex. In the hypothesis that the rejected traces are mainly due to neutral kaons decaying into two charged pions, for each pair of lines a secondary vertex is defined, by which a new momentum determination is obtained. Fig. 9 shows the invariant mass distribution for such pairs of tracks. A clean signal centered at the  $K^0$  mass is evident.

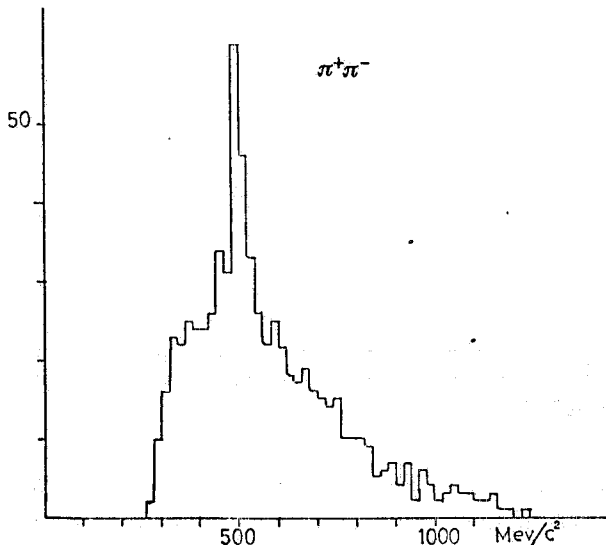


FIG. 9 - Invariant mass distribution of the reconstructed tracks pointing to the secondary vertexes.

#### 4. - CONCLUDING REMARKS

We built MWPC's with three sense planes, such that a single module can give a point in space without ambiguities, and where the ratio of useful surface to total surface is maximized. The chambers proved very reliable over a period of nearly one year of running. We did not observe any degradation of their operative characteristics. By the same period we had only one wire failure in about 3500 wires simultaneously working.

#### ACKNOWLEDGEMENTS

We would like to thank G. Corradi, L. Daniello, L. Passamonti and V. Russo for their invaluable help during test and running of these chambers. We also thank Prof. G. De Franceschi for many useful discussions.

#### REFERENCES

- (1) E. Albini et al.; Electronic mesurement of the lifetime of D++ mesons, To be published in Phys. Letters.
- (2) J. Lindsay et al.; CERN 74-12 (1974).
- (3) G. Bologna et al.; Nucl. Instr. & Meth. 178, 587 (1980).